

Computational models for the shuttling motion of the macrocycle in rotaxane-based molecular switches

Pipsa Hirva · Matti Haukka · Tapani A. Pakkanen

Received: 13 February 2008 / Accepted: 4 June 2008 / Published online: 5 July 2008
© Springer-Verlag 2008

Abstract The shuttling motion of a macrocycle in rotaxane-based molecular switching devices has been studied by computational density functional methods. In the test case, energy profiles corresponding to the dethreading process of different types of guest molecules in a cyclobis(paraquat-p-phenylene) host verified the experimental preference of the tetrathiafulvalene recognition site over the dioxynaphthalene site in a Stoddart-Heath type molecular device. Furthermore, modification of the redox state of either the macrocycle or the guest molecule resulted in considerable changes in the computational energy profiles, which can be utilized in explaining the behavior of the host-guest system. In order to study the effect of chemical oxidation/reduction in the guest molecule, we have investigated a prototypical shaft including two octahedral ruthenium complexes linked by a conjugated C₁₄ carbon chain, where the shuttling motion can be triggered by changing the electronic environment of the active complexes with ligand exchange reactions. The computational results also indicated effective communication between the macrocycle and the conjugated carbon chain, therefore showing the importance of non-covalent host-guest interactions in the control of the motion.

Keywords Density functional calculations · Host-guest systems · Molecular switch · Nanostructures

Introduction

The possibility of manufacturing controllable nanoscale devices has opened up an active area of research. It has been suggested that catenanes, rotaxanes, pseudorotaxanes and other similar inclusion complexes can be used to mimic macroscopic devices such as molecular switches on a molecular scale. The non-covalent nature of the complexes permits a piston-like movement of a guest molecule between two or more station positions. One of the best known systems is based on inclusion complexes of cyclobis(paraquat-p-phenylene), CBPQT⁴⁺, with different kinds of organic shafts. [1–6] Most detailed experimental [6, 7] and computational [8–15] information can be found on the Stoddart-Heath type rotaxane. In its catenane form, the ring-shaped host molecule CBPQT⁴⁺ is shuttling along bis-p-phenylene-34-crown-10 guest, modified to include two redox active stations, a tetrathiafulvalene (TTF) and a dioxynaphthalene (DNP) site. The structure and energetics of CBPQT⁴⁺ have also been computationally studied for other types of guests including small organic binding sites, such as benzidine and 4,4'-biphenol [16–19]. Additionally, CBPQT⁴⁺ macrocycle modified with pentacycloundecane unit has been studied by semiempirical PM3 calculations in order to describe the effect of cavity size in the formation of inclusion complexes [20, 21]. Semiempirical calculations have been utilized to investigate host-guest interactions in an α -cyclodextrin host and benzaldehyde and acetophenone guests [22]. Furthermore, neutral [2] rotaxanes have been introduced in order to avoid the complications caused by the highly charged species in CBPQT⁴⁺ rotaxanes [23]. The Stoddart-Heath type bistable [2] rotaxane has also been utilized as a principal building block for more

P. Hirva (✉) · M. Haukka · T. A. Pakkanen
Department of Chemistry, University of Joensuu,
B.O.Box 111, FI-80101 Joensuu, Finland
e-mail: pipsa.hirva@joensuu.fi

advanced structures forming artificial muscles [24] or nanovalves on mesoporous silica [25].

There are several means of triggering the function of the switch, by external electric field, by magnetically or mechanically applied forces, and by chemical, photochemical or electrochemical reactions [26–28]. The shuttling motion of the CBPQT⁴⁺ macrocycle can be obtained by changing the electrochemical environment of the system by oxidizing the TTF recognition site of the shaft molecule [6, 7], or by reducing the macrocycle [1, 26]. There are also examples of electrochemically or photochemically induced conformational or structural changes in the host-guest system, where for example *cis-trans* isomerization or hydrogen bond formation can cause the shuttling motion in the rotaxane [29–32]. An example of chemical control in the shuttling movement includes a switch consisting of a cyclodextrin ring and a shuttle containing dodecamethylene and 4,4'-bipyridinium units [33]. The control can be achieved by temperature and solvent changes. In another type of a chemically switchable system the shuttling of the dibenzo [24] crown-8 ether along a dumbbell component containing a secondary ammonium center and a 4,4'-bipyridinium unit can be obtained by deprotonation/reprotonation of the ammonium station in acid/base reactions [34]. Furthermore, Bonnet et al. have introduced catenanes including ruthenium complexes with polydentate nitrogen-containing ligands in one of the macrocycles. Visible-light irradiation has been shown to lead to ligand exchange reactions at the ruthenium center and subsequent coordination/decoordination of the shuttling macrocycle [35]. The hybrid catenanes based on transition metal-containing macrocycles [36] could provide additional control in modification of, for example, the redox properties of the switch.

The main goal of our work was to study in detail the shuttling motion and corresponding host-guest interactions in a chemically controlled molecular switch by computational DFT methods. A new type of a rotaxane-based model guest was investigated and the relative energies involved in the dethreading process were calculated. We have also studied the energetics of the Stoddart-Heath type rotaxane in order to test the performance of current DFT methods in the optimization procedure of such a large system.

Models

To test the computational methods, the Stoddart-Heath type redox-controlled molecular switch was selected, since it has been extensively studied both experimentally and computationally. The experimental structure of its catenane form is shown in Fig. 1 [7]. Because the computational requirements in DFT optimization for the whole system were too

large for testing purposes, we chose to examine separately the effect of the two recognition sites (DNP and TTF in Fig. 1b).

Several previous studies have shown drastic conformational changes in the inclusion complexes upon the shuttling process, which frequently leads to folding of the guest [11–13, 17, 32]. The inevitable complexity of the conformational space complicates both experimental and computational studies. To avoid this kind of folding and to constrain the conformational freedom, we based our model guest molecule on a rigid alkyne chain containing conjugated triple bonds. A similar approach has been adopted in a [2] rotaxane based on CBPQT⁴⁺ host, where the problem of different guest conformations was removed by introducing rigid arylolethynyl or butadiynyl spacers between the two active stations [37]. Another reason for selecting the conjugated system was the need to enhance the charge transfer from one binding site to another. A “through molecule” electron transfer has been found in a prototypical

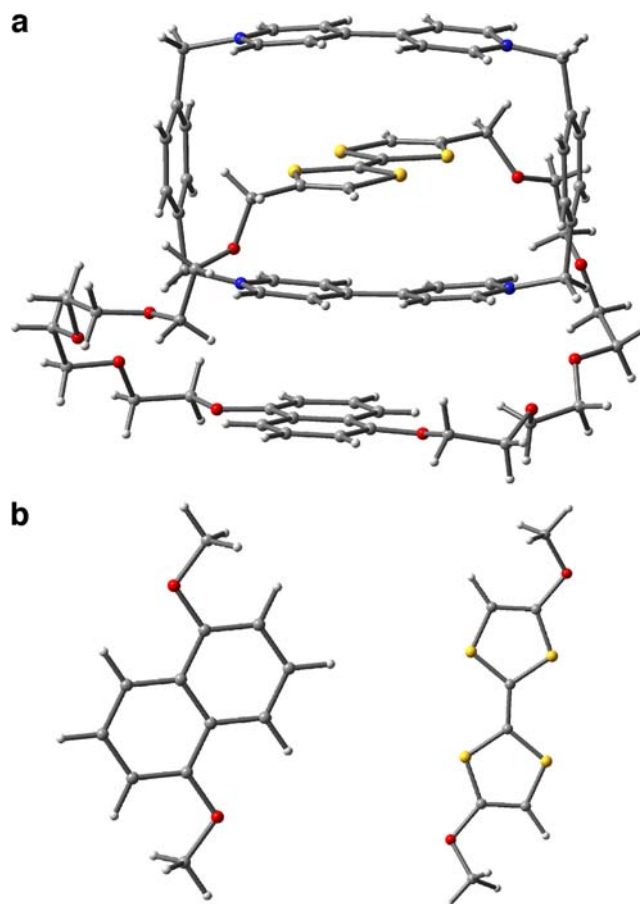


Fig. 1 a) Experimental X-ray structure of the [2]catenane of cyclobis(paraquat-p-phenylene) host and a modified bis-p-phenylene-34-crown-10 guest, modified to include two redox active stations, a tetrathiafulvalene (TTF) and a dioxynaphthalene (DNP) site [7]. b) models for the redox active recognition sites in the computational tests, DNP (left) and TTF (right)

conjugated molecular wire consisting of 1,4-bis(phenylethynyl)benzene units [38]. However, free rotation of the benzene rings very easily leads to an out-of-plane structure with hindered charge transfer. Therefore, we selected to study a guest with a $-C\equiv C-C\equiv C-$ linker between two redox active ruthenium complexes, similarly to a experimentally obtained $[\{Ru(dppe)Cp^*\}_2(\mu-C_{14})]$ [39].

As active end groups, we used octahedral ruthenium carbonyl complexes, which can undergo simple ligand exchange reactions. In the basic configuration, two Ru(II) $(CO)_3H-$ groups were linked together by the conjugated alkyne chain (NE, Fig. 2a). The Ru1 end of the guest was then chemically modified by exchanging the formally anionic hydride ligand with a neutral carbonyl ligand, leading to a cationic guest (CAT, Fig. 2b). In an opposite chemical reaction, one of the carbonyl ligands was exchanged to a hydride ligand (AN, Fig. 2c). It should be noted, that the pyridine ligand in the active complexes was merely added as a potential chromophoric component, to increase the possibilities for introducing energy in the system by photochemical means.

Computational methods

All calculations were done by the Gaussian 03 program package [40]. The energy profiles were obtained by constraining the distance (d) of the center of the guest molecule from the center of the cavity of the shuttling macrocycle host. All other geometrical parameters were fully optimized with SCF convergence criteria of 10^{-8} Hartrees. A nonlocal hybrid functional MPW1K [41] was selected for the computations, because this functional has been found to perform well especially in describing different kinds of non-

bonded interactions [42]. The basis set was the standard 6-31G(d) for other atoms than ruthenium, for which a Stuttgart-Dresden small core ECP [43] with an extra p-polarization function [44] was selected.

Results and discussion

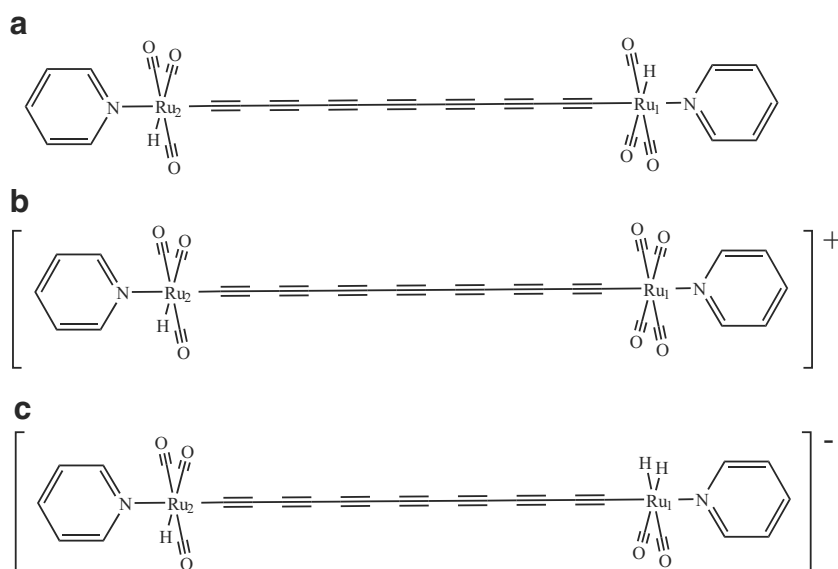
Energy profiles for the dethreading of the DNP and TTF guests

We calculated energy profiles of the dethreading process for the DNP and TTF guests (Fig. 1) in different redox conditions, to verify that the MPW1K functional is able to reproduce the experimental observation that the relative strength of the interaction between these two recognition sites can be affected by either reducing the shuttling macrocycle, or by oxidizing the TTF site. The energy profiles are shown in Fig. 3, where we have referenced the interaction energies to the corresponding free isolated species, to be able to compare the relative stability of the complexes.

In its normal oxidation state +4, CBPQT macrocycle interacts more strongly with the TTF binding site than with the DNP site, in accordance to the experimental and previous computational findings. Interestingly, the minimum energy structure for TTF is not the one, where the guest is symmetrically located at the center of the cavity. Instead, larger stabilization can be found at the dethreading distance of about 1.2–1.5 Å, where the sulfur atoms of the outgoing guest can interact with the aromatic rings of the macrocycle. Furthermore, the energy maximum for TTF guest is obtained at longer dethreading distances than for DNP, and it is also slightly higher, thus enhancing the favorability of the inclusion complex.

Fig. 2 The structure of the computationally designed guest.

a) neutral (NE) guest, **b)** cationic [CAT]⁺ guest, **c)** anionic [AN]⁻ guest



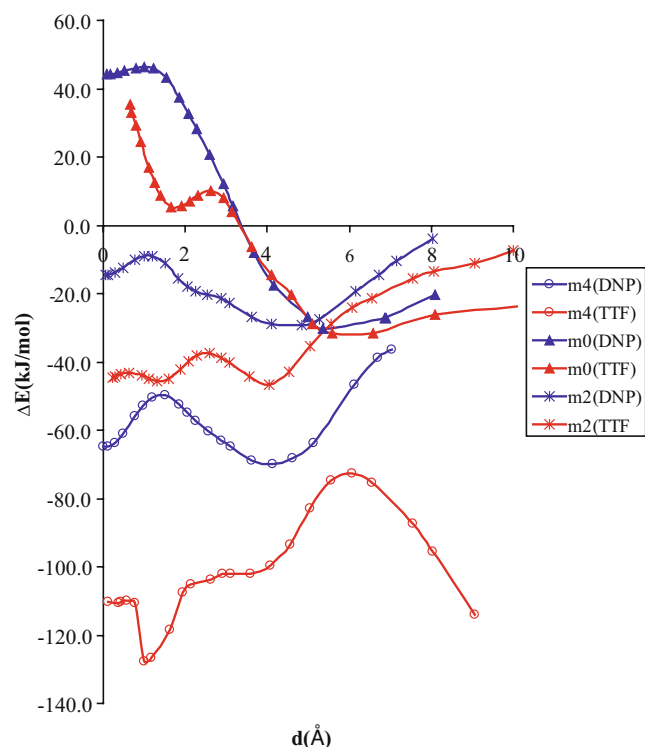


Fig. 3 The energy profiles for the dethreading process of the CBPQT^{n+} ($n=0,2,4$) with the two recognition sites, DNP (blue curves) and TTF (red curves). Notations m0, m2 and m4 represent the different oxidation states of the macrocycle ($m_0=0$, $m_2=+2$, $m_4=+4$). The parameter d represents the distance of the center of the guest molecules from the center of the cavity of the macrocycle

When the CBPQT macrocycle was reduced $+4 \Rightarrow +2 \Rightarrow 0$, two observations were made according to the energy profiles. First, the interaction between the macrocycle and the guest reduced considerably. Consequently, both of the guest molecules disfavored the formation of the inclusion complex, and were drawn away from the center of the cavity of the macrocycle. In fact, at lower oxidation states of the macrocycle it was not possible to optimize the structure of the TTF guest at the vicinity of the center. Secondly, although a small preference of the TTF guest is still seen at smaller dethreading distance, corresponding to the similar interaction of the sulphur atoms with the aromatic rings of the macrocycle than in the oxidation state $+4$, at longer dethreading distances all selectivity is lost and both guests show similar behavior with the same relative energy. This suggests, that reduction of the macrocycle will not be effective enough to trigger consistent change of the binding sites, and thus the shuttling motion of the macrocycle. It should be noted, that with larger distances ($d > 6$ Å), especially in the case of oxidation state $+4$, the CBPQT macrocycle experiences large changes in the torsions of the aromatic rings, which leads to additional

stabilization of the system. Extra stabilization is caused also by oxygen atoms in the guest "tails", which interact with the protons of the aromatic rings. Similar C-O-H interactions have been suggested to be an important contribution to the stabilization of the catenane structure presented in Fig. 1 [6]. However, our models are probably too short to give reliable energies at the longer dethreading distances.

Experimental observations have shown, that the shuttling motion can be obtained when instead of reducing the macrocycle, the TTF^0 binding site is oxidized to TTF^{2+} [6, 7, 15]. We compared the energy profiles of dethreading the TTF guest with both oxidations states. The results are shown in Fig. 4.

When the originally strongly interacting TTF^0 guest is oxidized to TTF^{2+} , host-guest interactions decrease and the guest is driven out from the center of the cavity of the macrocycle, which is exactly what is experimentally observed. Since the DNP binding site still remains neutral, it will form the inclusion complex with the macrocycle, and thus selective and reversible oxidation/reduction cycles of the TTF guest will lead to shuttling motion of the macrocycle.

Encouraged by the consistent results from the energy profiles of the existing rotaxane, we decided to further expand our studies into a new type of shuttling rotaxane, which could function as a molecular switch. Details of the modifications can be found in the Models section.

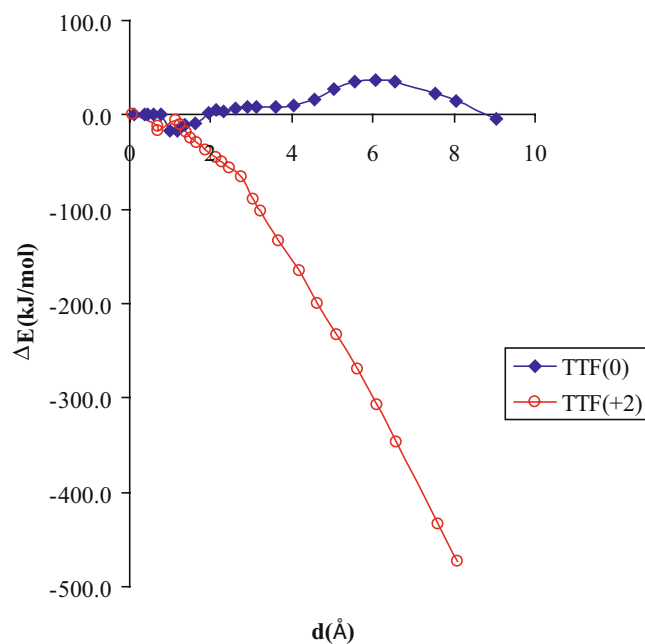


Fig. 4 Energy profiles of the dethreading process of the TTF^{n+} ($n=0,2$) guest from the CBPQT^{4+} macrocycle. The relative energies are referenced to the dethreading distance $d=0.0$ Å

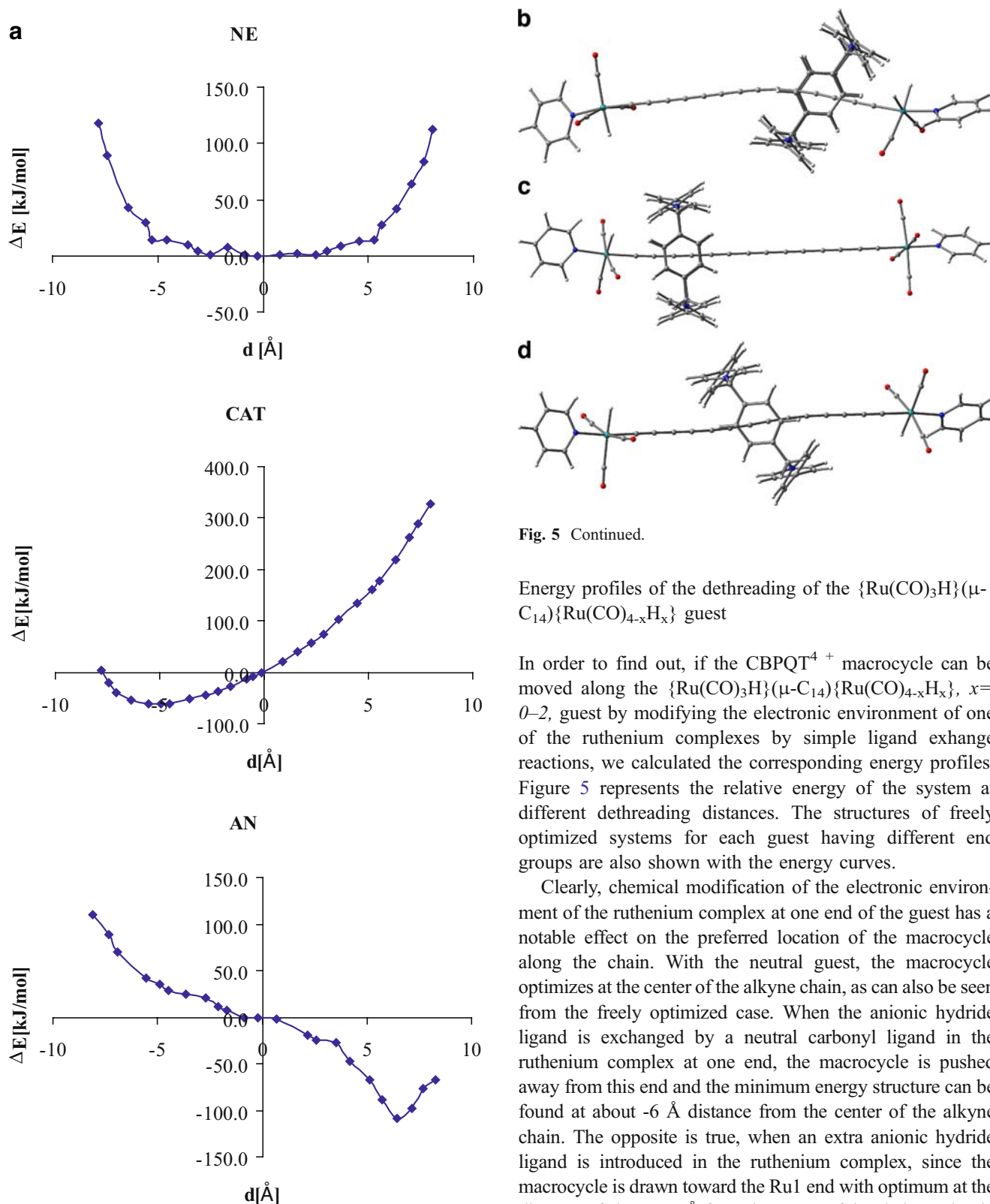


Fig. 5 **a**) The relative energy curves for the dethreading process of the $\{\text{Ru}(\text{CO})_3\text{H}\}(\mu\text{-C}_{14})\{\text{Ru}(\text{CO})_{4-x}\text{H}_x\}$, $x=0-2$, guest in the CBPQT^{4+} host. The pictures represent a side view of the freely optimized structure of the corresponding host-guest system, **b**) anionic (AN), **c**) cationic (CAT), **d**) neutral (NE) guest

Fig. 5 Continued.

Energy profiles of the dethreading of the $\{\text{Ru}(\text{CO})_3\text{H}\}(\mu\text{-C}_{14})\{\text{Ru}(\text{CO})_{4-x}\text{H}_x\}$ guest

In order to find out, if the CBPQT^{4+} macrocycle can be moved along the $\{\text{Ru}(\text{CO})_3\text{H}\}(\mu\text{-C}_{14})\{\text{Ru}(\text{CO})_{4-x}\text{H}_x\}$, $x=0-2$, guest by modifying the electronic environment of one of the ruthenium complexes by simple ligand exchange reactions, we calculated the corresponding energy profiles. Figure 5 represents the relative energy of the system at different dethreading distances. The structures of freely optimized systems for each guest having different end groups are also shown with the energy curves.

Clearly, chemical modification of the electronic environment of the ruthenium complex at one end of the guest has a notable effect on the preferred location of the macrocycle along the chain. With the neutral guest, the macrocycle optimizes at the center of the alkyne chain, as can also be seen from the freely optimized case. When the anionic hydride ligand is exchanged by a neutral carbonyl ligand in the ruthenium complex at one end, the macrocycle is pushed away from this end and the minimum energy structure can be found at about -6 Å distance from the center of the alkyne chain. The opposite is true, when an extra anionic hydride ligand is introduced in the ruthenium complex, since the macrocycle is drawn toward the Ru1 end with optimum at the distance of about $+6$ Å from the center of the chain. It should be noted, that especially in the AN case, modifying the ligand structure of the ruthenium complex results in substantial bending of the macrocycle and also the alkyne chain at larger dethreading distances, probably due to overestimation

Table 1 Selected NPA charges of the $\{\text{Ru}(\text{CO})_3\text{H}\}(\mu\text{-C}_{14})\{\text{Ru}(\text{CO})_{4-x}\text{H}_x\}$, $x=0-2$, guest

	Guest			Host + guest		
	NE	CAT	AN	NE	CAT	AN
Ru1	-0.390	-0.354	-0.374	-0.383	-0.361	-0.340
C11	-0.057	-0.226	0.111	0.116	-0.066	0.063
C12	-0.257	-0.125	-0.367	-0.352	-0.218	-0.412
C13	0.048	-0.041	0.130	0.135	0.132	0.032
C14	-0.086	0.018	-0.198	-0.227	-0.089	-0.185
C15	0.004	-0.058	0.064	0.006	0.106	-0.062
C16	-0.045	0.036	-0.147	-0.154	-0.092	-0.088
C17	-0.020	-0.071	0.026	-0.074	0.073	-0.140
C27	-0.020	0.049	-0.105	-0.075	-0.115	0.007
C26	-0.045	-0.089	-0.011	-0.153	-0.023	-0.162
C25	0.004	0.056	-0.064	0.005	-0.101	0.107
C24	-0.086	-0.120	-0.058	-0.227	-0.118	-0.168
C23	0.048	0.105	-0.005	0.134	0.001	0.174
C22	-0.257	-0.281	-0.230	-0.351	-0.334	-0.312
C21	-0.057	-0.007	-0.107	0.115	-0.060	0.078
Ru2	-0.390	-0.392	-0.387	-0.383	-0.372	-0.393

Numbering scheme: Ru1 = chemically modified ruthenium atom, C11 = carbon next to Ru1, C21 = carbon next to Ru2, other numbering follows the order in the conjugated C_{14} chain. Boxes indicate the position of the host along the carbon chain.

of the H-H interactions between the ruthenium complex and the aromatic rings of the macrocycle. With smaller hydride ligands, the macrocycle is also able to move closer to the end complex, and thus the energy does not rise as early as with the other complexes.

Charge transfer properties

One advance in the conjugated triple bond linker system is the “through molecule” charge transfer along the chain

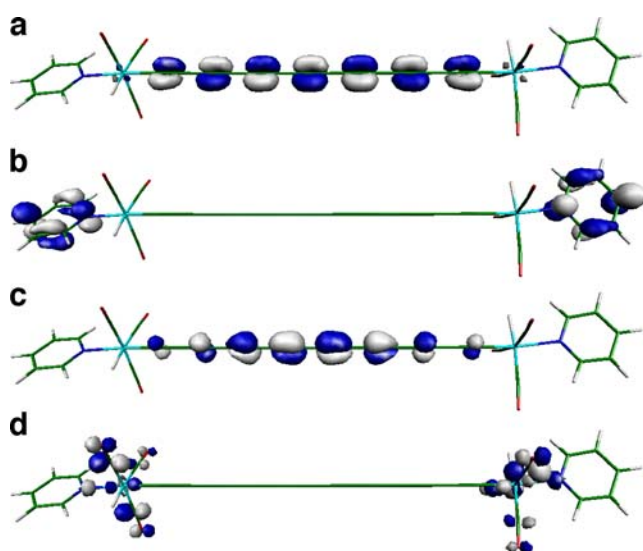


Fig. 6 Selected frontier molecular orbitals of the $\{\text{Ru}(\text{CO})_3\text{H}\}_2(\mu\text{-C}_{14})$ guest, **a**) HOMO, **b**) LUMO, **c**) LUMO+2, **d**) LUMO+4

from one end group to another. To study the charge transfer properties in our $\{\text{Ru}(\text{CO})_3\text{H}\}(\mu\text{-C}_{14})\{\text{Ru}(\text{CO})_{4-x}\text{H}_x\}$, $x=0-2$, guest, we calculated the NPA charge distribution within different guest configurations. Table 1 shows the charges of the guest molecules along the axle in separately optimized guests and in the host-guest systems.

When the separate guest is modified by changing the electronic environment of Ru1, the charge is not modified only at the Ru1 end, but it is distributed along the carbon chain. However, the resulting change is not very effectively seen at the Ru2 charge, which is only slightly modified. Due to non-bonding interactions of the macrocycle and the

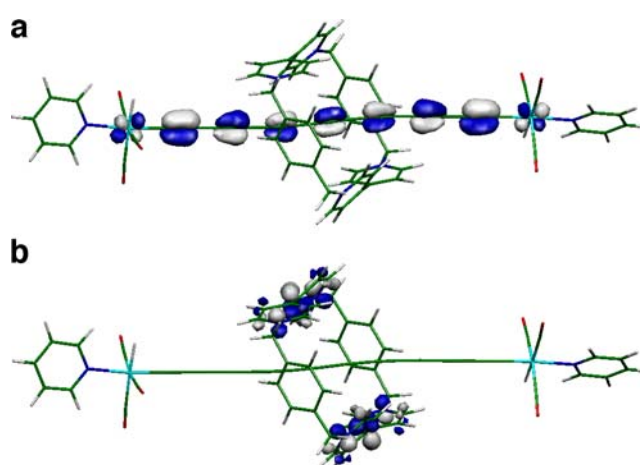


Fig. 7 Selected frontier molecular orbitals of the host-guest system with CBPQT⁴⁺ host and $\{\text{Ru}(\text{CO})_3\text{H}\}_2(\mu\text{-C}_{14})$ guest, **a**) HOMO, **b**) LUMO

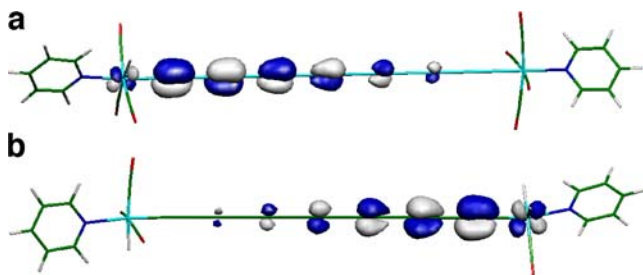


Fig. 8 HOMO orbitals for the a) cationic guest, b) anionic guest

guest molecule, the host donates charge distribution to the guest, and consequently, the charge of the carbon atoms in the vicinity of the host is more negative than in the separate guests. When the guest is chemically modified, changes at the electron density are reflected to the host-guest interactions, and thus the charge distribution of the system changes when the macrocycle is moving along the chain.

We sought a detailed description of the electronic properties of the host-guest systems by analyzing the effect of host-guest interactions on the frontier molecular orbitals. Examples of the orbitals in the $\{\text{Ru}(\text{CO})_3\text{H}\}_2(\mu\text{-C}_{14})$ guest are shown in Fig. 6, and in the host-guest system in Fig. 7.

The highest occupied molecular orbital (HOMO) is similar in both the separate guest and in the host-guest system. It is mainly formed from the π system of the conjugated carbon linker, with a contribution from the metal d-orbitals of the ruthenium complexes. However, there are large changes in the structure of the lowest unoccupied molecular orbital. The LUMO orbital and several following orbitals of the separate guest consist of the ligand system of the ruthenium ends (LUMO consists of pyridine orbitals, LUMO + 2 from C_{14} chain orbitals and LUMO + 4 of carbonyl ligand orbitals, for example). When the host-guest complex is formed, there is a substantial contribution of the macrocycle orbitals in the LUMO and the following higher orbitals, indicating notable interaction between the CBPQT^{4+} host and the $\{\text{Ru}(\text{CO})_3\text{H}\}_2(\mu\text{-C}_{14})$ guest.

Figure 8 shows the HOMO orbitals for the cationic and anionic guest molecules. In the cationic guest, the highest occupied molecular orbital loses its symmetric nature, and is concentrated in the vicinity of Ru2. The opposite is true with the anionic guest, and the HOMO concentrates in the vicinity of Ru1. This difference in the HOMO orbitals can explain the different optimized locations along the carbon chain, since it enables the strongest host-guest interactions between the HOMO of the guest and the LUMO of the host at different sites.

Conclusions

In the current study, we have modeled different host-guest systems by computational density functional methods. The

energy profiles of the dethreading process of a guest molecule in a cyclobis(paraquat-p-phenylene) macrocycle show, that the shuttling motion resulting from the modification of the redox properties of the organic or organometallic guests can be modeled by the MPW1K functional. Additional information on the energetic and geometrical changes at larger distances from the equilibrium state can also be obtained from the energy profiles. The information from the test calculations has been utilized in the investigation of a new model guest molecule, where chemical oxidation/reduction can be achieved by ligand exchange reactions. Naturally, it would be difficult to experimentally perform selective chemical reactions only at one end of the model guest without using different complexes as end groups (for example, large organic blocking ligands or different metal complexes). However, the simplified model will give detailed information on the charge transfer processes and therefore on the requirements needed to induce the movement of the macrocycle. At the next stage, the more subtle effects induced by varying the end groups can be studied by comparing the corresponding energy profiles.

Energy profiles for the dethreading process of the model host-guest system including a CBPQT^{4+} host and a $\{\text{Ru}(\text{CO})_3\text{H}\}(\mu\text{-C}_{14})\{\text{Ru}(\text{CO})_{4-x}\text{H}_x\}$, $x=0-2$, guest show notable changes in the preferred location of the macrocycle along the conjugated carbon chain, when simple ligand exchange reactions are performed at the active ruthenium centers. Therefore, modification of the electronic environment of the active sites in the guest molecule can be utilized to trigger the shuttling motion of the macrocycle.

The changes in the charge distribution and the frontier molecular orbitals in the $\{\text{Ru}(\text{CO})_3\text{H}\}_2(\mu\text{-C}_{14})$ guest upon the formation of the inclusion complex show effective communication through the conjugated triple bond system of the C_{14} chain and a notable contribution of the macrocycle, therefore showing the importance of non-covalent host-guest interactions in the control of the motion.

Acknowledgements Financial support from the Academy of Finland (P.H., M.H.) is gratefully acknowledged.

References

1. Anelli PL, Ashton PR, Ballardini R, Balzani V, Delgado M, Gandolfi MT, Goodnow TT, Kaifer AE, Philp D, Pietraszkiewicz M, Prodi L, Reddington MV, Slawin AMZ, Spencer N, Stoddart JF, Vicent C, Williams DJ (1992) *J Am Chem Soc* 114:193–218
2. Aprahamian I, Dichtel WR, Ikeda T, Heath JR, Stoddart JF (2007) *Org Lett* 9:1287–1290
3. Ballardini R, Balzani V, Dehaen W, Dell'Erba AE, Raymo FM, Stoddart JF, Venturi M (2000) *Eur J Org Chem* 591–602
4. Dichtel WR, Miljanic OS, Spruell JM, Heath JR, Stoddart JF (2006) *J Am Chem Soc* 128:10388–10390

5. Ikeda T, Aprahamian I, Stoddart JF (2007) *Org Lett* 9:1481–1484
6. Pease AR, Jeppesen JO, Stoddart JF, Luo Y, Collier CP, Heath JR (2001) *Acc Chem Res* 34:433–444
7. Asakawa M, Ashton PR, Balzani V, Credi A, Hamers C, Matternsteig G, Montaldi M, Shipway AN, Spencer N, Stoddart JF, Tolley MS, Venturi M, White AJP, Williams DJ (1998) *Angew Chem Int Ed* 37:333–337
8. Ceccarelli M, Mercuri F, Passerone D, Parrinello M (2005) *J Phys Chem B* 109:17094–17099
9. Deng W-Q, Muller RP, Goddard WA III (2004) *J Am Chem Soc* 126:13562–13563
10. Ercolani G, Mencarelli P (2003) *J Org Chem* 68:6470–6473
11. Jang SS, Jang YH, Kim Y-H, Goddard WA III, Choi JW, Heath JR, Laursen BW, Flood AH, Stoddart JF, Norgaard K, Bjornholm T (2005) *J Am Chem Soc* 127:14804–14816
12. Jang SS, Jang YH, Kim Y-H, Goddard WA III, Flood AH, Laursen BW, Tseng H-R, Stoddart JF, Jeppesen JO, Choi JW, Steuerman DW, Delonno E, Heath JR (2005) *J Am Chem Soc* 127:1563–1575
13. Jang YH, Hwang S, Kim Y-H, Jang SS, Goddard WA III (2004) *J Am Chem Soc* 126:12636–12645
14. Jang YH, Jang SS, Goddard WA III (2005) *J Am Chem Soc* 127:4959–4964
15. Jang YH, Goddard WA III (2006) *J Phys Chem B* 110:7660–7665
16. Grabuleda X, Jaime C (1998) *J Org Chem* 63:9635–9643
17. Grabuleda X, Ivanov P, Jaime C (2003) *J Phys Chem B* 107:7582–7588
18. Grabuleda X, Ivanov P, Jaime C (2003) *J Org Chem* 68:1539–1547
19. Kaminski GA, Jorgensen WL (1999) *J Chem Soc, Perkin Trans* 2:2365–2375
20. Castro R, Davidov PD, Kumar KA, Marchand AP, Evanseck JD, Kaifer AE (1997) *J Phys Org Chem* 10:369–382
21. Macias AT, Kumar KA, Marchand AP, Evanseck JD (2000) *J Org Chem* 65:2083–2089
22. Liu L, Li X-S, Song K-S, Guo Q-X (2000) *J Mol Struct (THEOCHEM)* 531:127–134
23. Iijima T, Vignon SA, Tseng HR, Jarrosson T, Sanders JKM, Marchioni F, Venturi M, Apostoli E, Balzani V, Stoddart JF (2004) *Chem Eur J* 10:6375–6392
24. Liu Y, Flood AH, Bonvallet PA, Vignon SA, Northrop BH, Tseng H-R, Jeppesen JO, Huang TJ, Brough B, Baller M, Magonov S, Solares SD, Goddard WA III, Ho C-M, Stoddart JF (2005) *J Am Chem Soc* 127:9745–9759
25. Nguyen TD, Liu Y, Saha S, Leung KCF, Stoddart JF, Zink JJ (2007) *J Am Chem Soc* 129:626–634
26. Ballardini R, Balzani V, Credi A, Gandolfi MT, Venturi M (2001) *Acc Chem Res* 34:445–455
27. Goldhaber-Gordon D, Montemerlo MS, Love JC, Opiteck GJ, Ellenbogen JC (1997) *Proc IEEE* 85:521–540
28. Shipway AN, Wilner I (2001) *Acc Chem Res* 34:421–432
29. Qu D-H, Wang Q-C, Ren J, Tian H (2004) *Org Lett* 6:2085–2088
30. Smukste I, Smithrud DB (2003) *J Org Chem* 68:2547–2558
31. Sohlberg K, Sumpter BGNDW (1999) *J Mol Struct (THEOCHEM)* 491:281–286
32. Zheng X, Sohlberg K (2003) *J Phys Chem A* 107:1207–1215
33. Harada A (2001) *Acc Chem Res* 34:456–464
34. Garaudee S, Silvi S, Venturi M, Credi A, Flood AH, Stoddart JF (2005) *Chem Phys Chem* 6:2145–2152
35. Bonnet S, Collin J-P, Koizumi M, Mobian P, Sauvage J-P (2006) *Adv Mater* 18:1239–1250
36. Chas M, Pia E, Toba R, Peinadir C, Quintela JM (2006) *Inorg Chem* 45:6117–6119
37. Nygaard S, Leung KCF, Aprahamian I, Ikeda T, Saha S, Laursen BW, Kim S-Y, Hansen SW, Stein PC, Flood AH, Stoddart JF, Jeppesen JO (2007) *J Am Chem Soc* 129:960–970
38. Beeby A, Findlay KS, Low PJ, Marder TB, Matousek P, Parker AW, Rutter SR, Towrie M (2003) *Chem Commun* 2406–2407
39. Antonova AB, Bruce MI, Ellis BG, Gaudio M, Humphrey PA, Jevric M, Melino G, Nicholson BK, Perkins JG, Skelton BW, Stapleton B, White AH, Zaitseva NN (2004) *Chem Commun* 960
40. Frisch MJ, Trucks GW, Schlegel HB, Scuseria GE, Robb MA, Cheeseman JR, Montgomery JA, Vreven T, Kudin KN, Burant JC, Millam JM, Iyengar SS, Tomasi J, Barone V, Mennucci B, Cossi M, Scalmani G, Rega N, Petersson GA, Nakatsuji H, Hada M, Ehara M, Toyota K, Fukuda R, Hasegawa J, Ishida M, Nakajima T, Honda Y, Kitao O, Nakai H, Klene M, Li X, Knox JE, Hratchian HP, Cross JB, Bakken V, Adamo C, Jaramillo J, Gomperts R, Stratmann RE, Yazyev O, Austin AJ, Cammi R, Pomelli C, Ochterski JW, Ayala PY, Morokuma K, Voth GA, Salvador P, Dannenberg JJ, Zakrzewski VG, Dapprich S, Daniels AD, Strain MC, Farkas O, Malick DK, Rabuck AD, Raghavachari K, Foresman JB, Ortiz JV, Cui Q, Baboul AG, Clifford S, Cioslowski J, Stefanov BB, Liu G, Liashenko A, Piskorz P, Komaromi I, Martin RL, Fox DJ, Keith T, Al-Laham MA, Peng CY, Nanayakkara A, Challacombe M, Gill PMW, Johnson B, Chen W, Wong MW, Gonzalez C, Pople JA, Gaussian 03, Revision C.02, Gaussian, Inc., Wallingford CT, 2004.
41. Lynch BJ, Fast PL, Harris M, Truhlar DG (2000) *J Phys Chem A* 104:4811–4815
42. Zhao Y, Truhlar DG (2005) *J Phys Chem A* 109:5656–5667
43. Basis sets were obtained from the Extensible Computational Chemistry Environment Basis Set Database, Version 02/02/06, as developed and distributed by the Molecular Science Computing Facility, Environmental and Molecular Sciences Laboratory which is part of the Pacific Northwest Laboratory, P.O. Box 999, Richland, Washington 99352, USA, and funded by the U.S. Department of Energy. The Pacific Northwest Laboratory is a multi-program laboratory operated by Battelle Memorial Institute for the U.S. Department of Energy under contract DE-AC06-76RLO 1830. Contact Karen Schuchardt for further information (2007)
44. Huzinaga S (ed.) (1984) *Gaussian Basis Sets for Molecular Calculations*. Physical Sciences Data 16, Elsevier, Amsterdam